

REF FILE COPY

2

MTL TR 90-59

AD

AD-A231 423

A COMPUTATIONALLY VIABLE HIGHER-ORDER THEORY FOR LAMINATED COMPOSITE PLATES

ALEXANDER TESSLER and ERIK SAETHER
MECHANICS AND STRUCTURES BRANCH

November 1990

Approved for public release; distribution unlimited.

DTIC
ELECTE
JAN 23 1991
S B D



US ARMY
LABORATORY COMMAND
MATERIALS TECHNOLOGY LABORATORY



U.S. ARMY MATERIALS TECHNOLOGY LABORATORY
Watertown, Massachusetts 02172-0001

The findings in this report are not to be construed as an official Department of the Army position, unless so designated by other authorized documents.

Mention of any trade names or manufacturers in this report shall not be construed as advertising nor as an official indorsement or approval of such products or companies by the United States Government.

DISPOSITION INSTRUCTIONS

Destroy this report when it is no longer needed.
Do not return it to the originator.

Block No. 20

ABSTRACT

A variational higher-order theory involving all transverse strain and stress components is proposed for the analysis of laminated composite plates. Derived from three-dimensional elasticity with emphasis on developing a viable computational methodology, the theory is well suited for finite element approximations as it incorporates both C^0 and C^1 continuous kinematic fields and Poisson boundary conditions. From the theory, a simple three-node stretching-bending finite element is developed and applied to the problem of cylindrical bending of a symmetric carbon/epoxy laminate for which an exact solution is available. Both the analytic and finite element results were found to be in excellent agreement with the exact solution for a wide range of the length-to-thickness ratio. The proposed higher-order theory has the same computational advantages as first-order shear-deformable theories. The present methodology, however, provides greater predictive capability, especially, for thick-section composites.

CONTENTS

1. INTRODUCTION	1
2. ANALYTIC BASIS OF HIGHER-ORDER PLATE THEORY	
2.1 Remark	11
3. FINITE ELEMENT DEVELOPMENT	
3.1 Thin-Regime Considerations	11
3.1.1 Three-Node Anisoparametric Interpolations	12
3.1.2 Shear Relaxation	13
4. TRANSVERSE STRESS CALCULATIONS	13
5. RESULTS AND DISCUSSION	15
6. CONCLUDING REMARKS	19
ACKNOWLEDGMENT	20
APPENDIX A. PLATE STRESS RESULTANTS AND STRAINS	21
APPENDIX B. PLATE CONSTITUTIVE RELATIONS	23
REFERENCES	25

Accession For	
NTIS GRA&I	<input checked="checked" type="checkbox"/>
DTIC TAB	<input type="checkbox"/>
Unannounced	<input type="checkbox"/>
Justification	
By	
Distribution/	
Availability Codes	
Dist	Avail and/or Special
A-1	

1. INTRODUCTION

In composite laminates made of high stiffness and strength fiber-reinforced plies, the deformation effects due to transverse shearing and transverse normal stretching can often be significant, especially in thick laminates and those subject to short wavelength loading. These effects are more pronounced in composites than in homogeneous materials due to their inherently high material compliancy in the transverse directions relative to the axial fiber direction. Furthermore, composite laminates exhibit much lower strength in the transverse directions and at the ply interfaces, thus being particularly susceptible to matrix cracking and delaminations.

The modeling of laminated composite plates and shells has been the subject of intensive research in the last two decades. Following the pioneering developments of Reissner,^{1,2} Hildebrand et al.,³ and Mindlin⁴ in the analytic treatment of homogeneous elastic plates, a great number of displacement-based, stress-based, and mixed formulations for application to laminate composites have been explored (e.g., refer to the recent review papers by Reissner,⁵ Reddy,⁶ Noor and Burton,⁷ and references therein). Reddy⁶ groups laminate theories into three general classes: (1) equivalent single-layer theories (two-dimensional); (2) layer-wise theories (two-dimensional); and (3) continuum-based theories (two- and three-dimensional). Of the three classes, the single-layer displacement theories are the simplest and most economical to use.

One commonly recognized drawback of the single-layer displacement theories, however, is that all six components of stress, obtained from constitutive relations, are discontinuous at the ply interfaces whereas, according to elasticity theory, only the inplane stresses are discontinuous and the transverse stresses maintain continuity across the laminate thickness. However, when the transverse stresses are obtained by integrating the elasticity equations of equilibrium,⁸ accurate stress distributions can be recovered. To resolve the issue of transverse stresses in a direct fashion, Reissner^{9,10} proposed a mixed variational principle which uses the three displacement components and three transverse stresses as the independent variables. Although from an analytic standpoint this approach appears to have some qualitative advantages; from a computational perspective it possesses the characteristic deficiency of all stress and mixed formulations¹¹ which has a relatively large number of stress parameters which need to be solved in order to obtain element stiffnesses with the implication of an additional and often significant computational cost. Thus, in large-scale applications and, particularly, in computationally intensive nonlinear analyses, the elements of choice are those that provide the best compromise between accuracy and computational cost, with the displacement-based theories emerging as the preferred framework. In what follows we narrow our focus on the single-layer displacement theories and propose a new theory which is specifically formulated with a view on the computational aspects of thin and thick composite laminates.

In a single-layer displacement-based theory, the basic assumption is that concerning the through-thickness approximations of the displacement components. The displacement components are expanded across the total laminate thickness with respect to the thickness coordinate. The expansion coefficients (or the plate/shell kinematic variables) are functions of the inplane coordinates (and time, in dynamics). Commonly, the inplane displacements are expanded with a polynomial of the same degree, m , whereas the transverse displacement expansion may be of the different degree, n . Thus, the notation $\{m, n\}$ may be conveniently used to distinguish between the various single-layer theories.

The simplest and most extensively explored approximation is $\{1, 0\}$ (i.e., a linear inplane displacement and a constant transverse displacement, totaling five kinematic variables) or what is often referred to as the first-order shear deformable theories.¹²⁻¹⁴ These theories, which are extensions of the Mindlin theory,⁴ enforce zero transverse normal deformation by virtue of $n = 0$. When formulated from the principle of virtual work, the resulting two-dimensional variational principle requires only C^0 continuous kinematic fields, thus providing a convenient framework for developing simple and computationally efficient finite elements.¹⁵⁻¹⁹

Other developments have focused on higher-order theories; those which include transverse shear and disregard transverse normal deformations $\{m > 1, 0\}$,⁶ and those that account for both transverse shear and transverse normal deformations $\{m \geq 1, n \geq 2\}$, with the latter class of theories being less prevalent.²⁰⁻²² Although, in general, higher-order theories provide more accurate approximations of the laminate deformations, strains and stresses, they have not been particularly suited toward finite element approximations due to the presence of one or more limitations such as: (1) incorporating a large number of kinematic variables requiring C^0 or higher continuity; (2) imposing natural edge-boundary conditions that involve such non-classical quantities as higher-order stress resultants; and (3) the inability to model appropriate transverse stress boundary conditions at the top and bottom laminate surfaces. Other common deficiencies include the requirement of "shear correction" factors that tune the transverse shearing properties,^{20,21} and some theories lack a variational basis.²³

Recently, Tessler²⁴⁻²⁶ has developed a higher-order $\{1, 2\}$ theory for homogeneous plates which incorporates "field-consistent" transverse strains and is devoid of all aforementioned limitations. The novel feature of that theory is a displacement variational principle requiring only C^0 and C^1 continuity for the plate kinematic variables, which allows the development of efficient plate finite elements having an expanded applicability range. One such element, a three-node triangle with five engineering degrees-of-freedom (dof) at each node,²⁴ has demonstrated the same computational efficiency as its Mindlin counterpart.¹⁵ In this paper, an extension of this theory to laminated composite plates and the derivation of an efficient three-node plate finite element are presented.

In Section 2, the development of the $\{1, 2\}$ laminate plate theory from three-dimensional elasticity is presented. This is achieved by expanding the three Cartesian displacements in terms of the thickness coordinate using linear and parabolic distributions for the inplane and transverse displacements. Additionally, independent expansions are used for the transverse strains. By requiring exact transverse stress boundary conditions at the top and bottom plate faces and the independent transverse strains to have equivalent mean values to those obtained from the assumed displacements directly, improved expressions for the transverse shear and transverse normal strains are obtained. Employing the three-dimensional virtual work principle yields a set of seven partial differential equations of equilibrium and exclusively Poisson boundary conditions. The theory reduces to one of coupled 10th-order stretching-bending and 0th-order transverse stretching.

In Section 3, a three-node plate element based on the displacement variational statement of Section 2 is developed. There are seven kinematic variables in the formulation; however, because the two higher-order displacement variables do not have spatial gradients in the variational statement, they are assumed to be uniform within the element domain (C^1 continuous) and are statically condensed out at the element level. The inplane membrane displacements are assumed to vary linearly across the element while the bending variables are interpolated

using anisoparametric shape functions.¹⁵ Each element node has five engineering dof involving three displacements and two normal rotations. The transverse shear relaxation parameter¹⁶ is also employed to completely eliminate shear locking in the thin regime.

In Section 4, there is a brief discussion on the computation of accurate through-thickness distributions of the transverse stresses via a global smoothing technique.²⁷⁻²⁸ In Section 5, analytic and finite element solutions to the problem of cylindrical bending of a symmetric carbon/epoxy laminate are presented. Results are compared with Pagano's exact elasticity solution.²⁹ In Section 6, concluding remarks regarding the merits of the present composite plate analysis are presented.

2. ANALYTIC BASIS OF HIGHER-ORDER PLATE THEORY

The present theory is developed in the following manner: the Cartesian displacement components u_i ($i = x, y, z$) are expanded with respect to the dimensionless thickness coordinate $\xi = z/h \in [-1, 1]$, where u_z has the special parabolic form:

$$u_x(x, y, z) = u(x, y) + h\xi\theta_y(x, y) \quad (a)$$

$$u_y(x, y, z) = v(x, y) + h\xi\theta_x(x, y) \quad (b) \quad (1)$$

$$u_z(x, y, z) = w(x, y) + \xi w_1(x, y) + (\xi^2 + C)w_2(x, y) \quad (c)$$

where $\xi = 0$ designates the position of the middle surface S_m , $2h$ is the total plate thickness and C is a constant which makes $w(x, y)$ a weighted-average transverse displacement defined in accordance with Reissner,² that is,

$$w = \frac{3}{4h} \int_{-h}^h u_z(1 - \xi^2) dz \quad (2)$$

Substituting Equation 1c into Equation 2 and solving for C results in*

$$C = -1/5 \quad (2a)$$

The expansion coefficients of the inplane displacements u, v, θ_x, θ_y are also defined as weighted-average kinematic variables:

$$u = \frac{1}{2h} \int_{-h}^h u_x dz, \quad v = \frac{1}{2h} \int_{-h}^h u_y dz \quad (3)$$

$$\theta_x = \frac{3}{2h^3} \int_{-h}^h u_y z dz, \quad \theta_y = \frac{3}{2h^3} \int_{-h}^h u_x z dz \quad (4)$$

*The present notation for w_2 differs from that in Reference 24 by a factor of $2/3$.

where u and v denote the midplane displacements along the x and y directions, respectively, with θ_x and θ_y denoting rotations of a transverse normal about the x and y axes, respectively (see Figure 1).

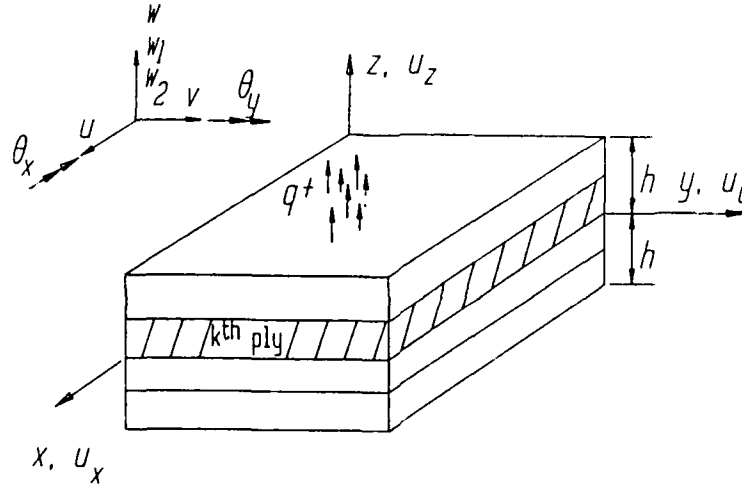


Figure 1. Plate notation

For a general composite layup composed of N plies, the stress-strain relation for each individual k^{th} ply ($k = 1, 2, \dots, N$) is governed by a three-dimensional Hooke's Law of the monoclinic form:

$$\begin{bmatrix} \sigma_{xx} \\ \sigma_{yy} \\ \sigma_{zz} \\ \tau_{yz} \\ \tau_{xz} \\ \tau_{xy} \end{bmatrix}^{(k)} = \begin{bmatrix} \tilde{C}_{11} & \tilde{C}_{12} & \tilde{C}_{13} & 0 & 0 & \tilde{C}_{16} \\ & \tilde{C}_{22} & \tilde{C}_{23} & 0 & 0 & \tilde{C}_{26} \\ & & \tilde{C}_{33} & 0 & 0 & \tilde{C}_{36} \\ & & & \tilde{C}_{44} & \tilde{C}_{45} & 0 \\ & & & & \tilde{C}_{55} & 0 \\ & & & & & \tilde{C}_{66} \end{bmatrix}^{(k)} \begin{bmatrix} \epsilon_{xx} \\ \epsilon_{yy} \\ \epsilon_{zz} \\ \gamma_{yz} \\ \gamma_{xz} \\ \gamma_{xy} \end{bmatrix} \quad (5)$$

(Sym.)

where the elastic constants $\tilde{C}_{ij}^{(k)}$ corresponding to the laminate x - y coordinates are related to the ply principal direction constants $C_{ij}^{(k)}$ as

$$\tilde{C}_{ij}^{(k)} = \alpha_{im} \alpha_{jn} C_{mn}^{(k)} \quad (6)$$

with α_{ij} denoting the appropriate cosine functions of the coordinate rotation between the ply principal material directions and laminate coordinates.³⁰

The inplane strain-displacement relations are obtained in the usual manner as,

$$\begin{aligned}\{\epsilon_{xx}, \epsilon_{yy}, \gamma_{xy}\} &= \{u_{x,x}, u_{y,y}, u_{x,y} + u_{y,x}\} \\ &= \{\epsilon_{x_0} + h\xi \kappa_{x_0}, \epsilon_{y_0} + h\xi \kappa_{y_0}, \gamma_{xy_0} + h\xi \kappa_{xy_0}\} \\ &= \{u_{,x} + h\xi \theta_{y,x}, v_{,y} + h\xi \theta_{x,y}, u_{,y} + v_{,x} + h\xi (\theta_{x,x} + \theta_{y,y})\}\end{aligned}\quad (7a)$$

A major departure from a conventional displacement formulation is the way the transverse strains are introduced into the theory. Here, the transverse strains are expanded independently in a field-consistent polynomial form,^{24,*}

$$\epsilon_{zz} = \sum_{n=0}^3 \xi^n a_n, \quad \gamma_{iz} = \sum_{n=0}^2 \xi^n b_{in} \quad (i=x,y) \quad (7b)$$

The expansion coefficients a_n and b_{in} are obtained by requiring the weak transverse strain compatibility

$$\text{minimize} \quad \int_{-h}^h \left[\epsilon_{zz} - u_{z,z} \right]^2 dz \quad (8a)$$

$$\text{minimize} \quad \int_{-h}^h \left[\gamma_{iz} - u_{z,i} - u_{i,z} \right]^2 dz \quad (i=x,y) \quad (8b)$$

*The approach of expanding the displacement gradients $u_{i,z}$ ($i = x, y, z$) introduced in Reference 24 is equivalent to the present one based on the transverse strain expansions.

and the satisfaction of the exact stress boundary conditions at the top ($k = N$) and bottom ($k = 1$) plate faces

$$\tau_{iz}^{(1)}(x,y,-h) = \tau_{iz}^{(N)}(x,y,h) = 0 \quad (i=x,y) \quad (9a)$$

$$\sigma_{zz,z}^{(1)}(x,y,-h) = \sigma_{zz,z}^{(N)}(x,y,h) = 0 \quad (9b)$$

where the minimization in Equation 8 is performed with respect to the unknown expansion coefficients. While Equation 9a is the statement of zero shear tractions at the top/bottom plate faces, Equation 9b results from the transverse equilibrium equation of three-dimensional elasticity

$$\tau_{xz,x}^{(k)} + \tau_{yz,y}^{(k)} + \sigma_{zz,z}^{(k)} = 0 \quad (\text{ignoring the body force}) \quad (10)$$

in which conditions Equation 9a are incorporated.

The resulting transverse shear strains have the parabolic distribution satisfying traction-free boundary conditions

$$\begin{aligned} \gamma_{iz} &= \frac{5}{4} (1 - \xi^2) \gamma_{iz_0} \quad (i=x,y) \\ \{\gamma_{xz_0}, \gamma_{yz_0}\} &= \{w_{,x} + \theta_y, w_{,y} + \theta_x\} \end{aligned} \quad (11)$$

which agree with Reissner's transverse shear strains.^{1,2}

The resulting cubic transverse normal strain can be written as

$$\epsilon_{zz} = \epsilon_{z_0} + \kappa^T \phi, \quad (12)$$

where

$$\epsilon_{z_0} = w_1/h$$

$$\kappa^T = (\kappa_{x_0}, \kappa_{y_0}, \kappa_{z_0}, \kappa_{xy_0}) = (\theta_{y,x}, \theta_{x,y}, w_2/h^2, \theta_{x,x} + \theta_{y,y})$$

$$\phi(\xi)^T = \{\phi_1, \phi_2, \phi_3, \phi_6\}$$

in which

$$\begin{aligned}\phi(\xi)_i &= \frac{h}{6} \{P_2(\xi) r_i - \frac{42}{85} [P_1(\xi)/14 + P_3(\xi)] s_i\} \\ r_i &= (\bar{C}_{31}/\bar{C}_{33})^{(k=1)} - (\bar{C}_{31}/\bar{C}_{33})^{(k=N)} \\ s_i &= (\bar{C}_{31}/\bar{C}_{33})^{(k=1)} + (\bar{C}_{31}/\bar{C}_{33})^{(k=N)} \quad (i=1,2,6).\end{aligned}$$

For $i = 3$,

$$\phi(\xi)_3 = \frac{28}{85} h [6P_1(\xi) - P_3(\xi)]$$

where $P_i(\xi)$ denote Legendre polynomials:

$$P_1(\xi) = \xi, \quad P_2(\xi) = (3\xi^2 - 1)/2, \quad P_3(\xi) = \xi(5\xi^2 - 3)/2$$

It can readily be verified that for a homogeneous plate Equations 11 and 12 satisfy the three-dimensional equilibrium Equation 10 exactly.

The plate equations of equilibrium together with the natural boundary conditions are obtained from the three-dimensional statement of virtual work[†] which, neglecting body forces, may be written as:

$$\begin{aligned}& \iiint_V (\sigma_{xx}^{(k)} \delta \epsilon_{xx} + \sigma_{yy}^{(k)} \delta \epsilon_{yy} + \sigma_{zz}^{(k)} \delta \epsilon_{zz} + \tau_{xy}^{(k)} \delta \gamma_{xy} + \tau_{xz}^{(k)} \delta \gamma_{xz} + \tau_{yz}^{(k)} \delta \gamma_{yz}) dV \\& - \iint_{S^+} q^+ \delta u_z(x, y, h) dx dy + \iint_{S^-} q^- \delta u_z(x, y, -h) dx dy \\& - \iint_{\partial \sigma} (\bar{T}_x \delta u_x + \bar{T}_y \delta u_y + \bar{T}_z \delta u_z) ds dz = 0\end{aligned}\tag{13}$$

[†]The statement can be regarded as a "weak" form of the virtual work principle due to the use of the mean compatibility requirement for the transverse strains (see Equation 8).

where δ is the variational operator; S^+ and S^- denote the top and bottom plate surfaces which are taken free of shear tractions and loaded by normal pressures,

$$\begin{aligned}\tau_{iz}^{(N)}(x,y,h) &= 0 \quad (i=x,y), \quad \sigma_{zz}^{(N)}(x,y,h) = q^+(x,y) \quad \text{on } S^+ \\ \tau_{iz}^{(1)}(x,y,-h) &= 0 \quad (i=x,y), \quad \sigma_{zz}^{(1)}(x,y,-h) = q^-(x,y) \quad \text{on } S^- \end{aligned} \quad (14)$$

where \bar{T}_i ($i = x, y, z$) denote the prescribed tractions on the part of the edge boundary S_σ (henceforth, the barred symbols will denote quantities prescribed at the plate edges). Integrating Equation 13 across the plate thickness results in the two-dimensional plate virtual work principle

$$\begin{aligned} & \iint_{S_m} \left\{ N_x \delta u_{,x} + N_y \delta v_{,y} + N_{xy} (\delta u_{,y} + \delta v_{,x}) + N_z \delta (w_1/h) \right. \\ & \quad + M_x \delta \theta_{y,x} + M_y \delta \theta_{x,y} + M_{xy} (\delta \theta_{x,x} + \delta \theta_{y,y}) + M_z \delta (w_2/h^2) \\ & \quad \left. + Q_x (\delta w_{,x} + \delta \theta_{y,y}) + Q_y (\delta w_{,y} + \delta \theta_{x,x}) \right\} dx dy \\ & - \iint_{S_m} \left\{ q_1 (\delta w + \frac{4}{5} \delta w_2) + q_2 \delta w_1 \right\} dx dy \\ & - \oint_{C_\sigma} \left\{ \bar{N}_{xn} \delta u + \bar{N}_{yn} \delta v + \bar{M}_{xn} \delta \theta_y + \bar{M}_{yn} \delta \theta_x + \bar{Q}_{zn} \delta w + \bar{Q}_{z_1} \delta w_1 + \bar{Q}_{z_2} \delta w_2 \right\} ds = 0 \end{aligned} \quad (15)$$

where the plate stress resultants are defined in Appendix A. Integrating Equation 15 by parts results in

$$\begin{aligned} & \iint_{S_m} \left\{ -[N_{x,x} + N_{xy,y}] \delta u - [N_{y,y} + N_{xy,x}] \delta v \right. \\ & \quad + [-M_{x,x} - M_{xy,y} + Q_x] \delta \theta_y + [-M_{y,y} - M_{xy,x} + Q_y] \delta \theta_x \\ & \quad - [Q_{x,x} + Q_{y,y} + q_1] \delta w + [N_z/h - q_2] \delta w_1 \\ & \quad \left. + [M_z/h^2 - \frac{4}{5} q_1] \delta w_2 \right\} dx dy \end{aligned}$$

$$\begin{aligned}
& + \oint_{C_\sigma} \left\{ (N_{xn} - \bar{N}_{xn}) \delta u + (N_{yn} - \bar{N}_{yn}) \delta v + (M_{xn} - \bar{M}_{xn}) \delta \theta_y + (M_{yn} - \bar{M}_{yn}) \delta \theta_x \right. \\
& \quad \left. + (Q_{zn} - \bar{Q}_{zn}) \delta w + \bar{Q}_{z_1} \delta w_1 + \bar{Q}_{z_2} \delta w_2 \right\} ds \\
& + \oint_{C_u} \left\{ N_{xn} \delta u + N_{yn} \delta v + M_{xn} \delta \theta_y + M_{yn} \delta \theta_x + Q_{zn} \delta w \right\} ds = 0
\end{aligned} \tag{16}$$

where

$$\begin{aligned}
N_{xn} &= N_x n_x + N_{xy} n_y, \quad N_{yn} = N_{xy} n_x + N_y n_y, \quad Q_{zn} = Q_x n_x + Q_y n_y, \\
M_{xn} &= M_x n_x + M_{xy} n_y, \quad M_{yn} = M_{xy} n_x + M_y n_y
\end{aligned} \tag{17}$$

and

$$\{n_x, n_y\} = \{\cos(x, n), \cos(y, n)\}$$

where the C_σ and C_u are parts of the boundary C ($C_u \cup C_\sigma = C$ and $C_u \cap C_\sigma = \emptyset$) surrounding the middle surface S_m where the tractions and displacements are prescribed; and n and s denoting the outward normal and tangential coordinates.

Thus, the variational principle provides seven equations of equilibrium written as:

$$(\delta u): \quad N_{x,x} + N_{xy,y} = 0 \tag{18a}$$

$$(\delta v): \quad N_{xy,x} + N_{y,y} = 0 \tag{18b}$$

$$(\delta \theta_y): \quad M_{x,x} + M_{xy,y} - Q_x = 0 \tag{18c}$$

$$(\delta \theta_x): \quad M_{xy,x} + M_{y,y} - Q_y = 0 \tag{18d}$$

$$(\delta w): \quad Q_{x,x} + Q_{y,y} + q_1 = 0 \tag{18e}$$

$$(\delta w_1): \quad N_z/h - q_2 = 0 \tag{18f}$$

$$(\delta w_2): \quad M_z/h^2 - \frac{4}{5} q_1 = 0 \tag{18g}$$

and the associate boundary conditions:

(a) Poisson boundary conditions

$$N_{xn} = \bar{N}_{xn}, \quad N_{yn} = \bar{N}_{yn}, \quad M_{xn} = \bar{M}_{xn}, \quad M_{yn} = \bar{M}_{yn}, \quad Q_{zn} = \bar{Q}_{zn} \quad \text{on } C_\sigma \quad (19)$$

(b) Vanishing higher-order shear resultants

$$\bar{Q}_{z_1} = \bar{Q}_{z_2} = 0 \quad \text{on } C_\sigma \quad (20)$$

(c) Displacement boundary conditions

$$u = \bar{u}, \quad v = \bar{v}, \quad \theta_y = \bar{\theta}_y, \quad \theta_x = \bar{\theta}_x, \quad w = \bar{w} \quad \text{on } C_u \quad (21)$$

The plate constitutive equations relating stress resultants to strains are summarized in Appendix B. Upon their introduction into Equation 18 there result two sets of equilibrium equations in terms of displacement variables:

$$Q_a L_{a2} u = L_{a1} q \quad (22)$$

$$w = R_b L_{b1} u + S_b q \quad (23)$$

where

$$q^T = \{q_1, q_2\}, \quad u^T = \{u, v, w, \theta_x, \theta_y\} \quad \text{and} \quad w^T = \{w_1, w_2\} \quad (24)$$

The Q_a , R_b , and S_b are various stiffness coefficient matrices. The L_{a1} and L_{b1} are first-order linear differential operators, and the L_{a2} is a second-order linear differential operator. The explicit forms of these matrix operators are rather cumbersome and, for this reason, they are not presented here. Note that Equation 22 contains five second-order coupled partial differential equations of equilibrium in the five displacement functions u , v , w , θ_x and θ_y (i.e., a 10th-order system), whereas Equation 23 has two zero-order equations in the w_1 and w_2 displacements.

The solution to a typical plate boundary-value problem is obtained by solving Equation 22 for u subject to the boundary conditions of Equations 19 and 21, and then solving the "auxiliary" system of Equation 23 for w . The computation of stress resultants follows from the plate constitutive equations (Appendix B), while the stresses are computed from the three-dimensional Hooke's Law in Equation 5. In Section 4, there is a brief discussion of an alternative procedure for recovering accurate transverse shear stresses.

2.1 Remark

The plate theory can be reduced to a shear-deformable one by enforcing infinite rigidity in the transverse normal material direction ($C_{33} = \infty$) and setting $C_{13} = C_{23} = 0$. Furthermore, with the additional assumption of infinite rigidity in the transverse shear directions ($C_{44} = C_{55} = \infty$), the theory yields results of the classical laminate plate theory (see Section 5).

3. FINITE ELEMENT DEVELOPMENT

The particular form of the variational principle (see Equation 15) lends itself well to the development of simple and efficient finite elements comparable in computational efficiency to the first-order shear-deformable elements.¹⁵⁻¹⁸ Recognizing that Equation 15 contains gradients of u , v , w , θ_x and θ_y that do not exceed order one implies C^0 continuity of these variables. In addition, Equation 15 has no gradients of w_1 and w_2 ; therefore, C^{-1} continuous approximations, which are discontinuous at the element boundaries, can be employed for these variables.

An important simplification due to w_1 and w_2 being C^{-1} continuous is that their dof can be conveniently eliminated at the element level via static condensation. Alternatively, the elimination of w_1 and w_2 can be performed in the variational statement by realizing that in Equation 15 the grouped terms associated with the arbitrary variations δw_1 and δw_2 must vanish independently. The result is Equation 18f and Equation 18g which, by using the constitutive relations for N_z and M_z (Appendix B), can be readily solved for w_1 and w_2 ; these are then replaced into Equation 15 prior to the finite element approximation. With this approach, Equation 18f and Equation 18g are satisfied exactly whereas the static condensation at the finite element level accomplishes the same purpose consistent with the finite element approximations.

3.1 Thin-Regime Considerations

By expressing Equation 15 in dimensionless form, it can further be shown that this variational principle is of a penalty-constraint type analogous to that of the Mindlin theory (e. g., refer to Reference 18). In the thin regime as $h \rightarrow 0$, it enforces the Kirchhoff constraint of the vanishing transverse shear angles, that is

$$\{\gamma_{xz_0}, \gamma_{yz_0}\} = \{w_{,x} + \theta_y, w_{,y} + \theta_x\} \rightarrow 0 \quad (25)$$

and the inextensibility of the transverse normal

$$w_1, w_2 \rightarrow 0$$

(26)

Whereas Equation 26 imposes no restrictions upon element interpolations for w_1 and w_2 , the Kirchhoff constraints (see Equation 25) require field consistency in the interpolations for w , θ_x and θ_y which may be achieved through the use of anisoparametric shape functions.¹⁵⁻¹⁸ In addition, an element-level relaxation of the transverse shear penalty parameter may be necessary when the field consistency is violated; for example, when excessive kinematic boundary restraints exist.¹⁶

In what follows, anisoparametric interpolations for a three-node element are summarized, and a brief discussion on the implementation of shear relaxation is presented. To distinguish element approximations from their analytic counterparts, the former are superscribed with an ℓ which, in the present notation, signifies a characteristic length scale of the discretization.

3.1.1 Three-Node Anisoparametric Interpolations

$$\left. \begin{aligned} u^\ell(x,y) &= \sum_{i=1}^3 \zeta_i u_i^\ell, & v^\ell(x,y) &= \sum_{i=1}^3 \zeta_i v_i^\ell \\ \theta_x^\ell(x,y) &= \sum_{i=1}^3 \zeta_i \theta_{xi}^\ell, & \theta_y^\ell(x,y) &= \sum_{i=1}^3 \zeta_i \theta_{yi}^\ell \end{aligned} \right\} \begin{array}{l} C^0 \text{ Linear} \\ \text{Shape} \\ \text{Functions} \end{array} \quad (27)$$

where ζ_i are the area-parametric coordinates given as

$$\zeta_i = (c_i + b_i x + a_i y)/2A \quad (A \text{ is the triangle area})$$

and a_i , b_i , and c_i are coefficients of nodal coordinates

$$a_i = x_k - x_j, \quad b_i = y_j - y_k, \quad c_i = x_j y_k - x_k y_j$$

$$\begin{aligned} w^\ell(x,y) &= \sum_{i=1}^3 [\zeta_i w_i^\ell + \theta_{xi}^\ell (b_k N_{i+3} - b_j N_{k+3})/8 \\ &\quad + \theta_{yi}^\ell (a_j N_{k+3} - a_k N_{i+3})/8] \end{aligned} \quad \begin{array}{l} C^0 \text{ Quadratic} \\ \text{Shape} \\ \text{Function} \end{array} \quad (28)$$

where N_i are quadratic shape functions

$$N_i = \zeta_i (2\zeta_i - 1), \quad N_{i+3} = 4\zeta_i \zeta_j$$

and the subscripts assume the values:

$$i = 1, 2, 3; \quad j = 2, 3, 1; \quad k = 3, 1, 2.$$

$$\left. \begin{aligned} w_1^L(x, y) &= W_1^L \\ w_2^L(x, y) &= W_2^L \end{aligned} \right\} \begin{array}{c} C^{-1} \text{ Uniform} \\ \text{Functions} \end{array} \quad (29)$$

Introducing Equations 27 through 29 into Equation 15, and performing the necessary variations with respect to the displacement dof and integrating over the element domain, the element stiffness equilibrium equations are derived. The W_1^L and W_2^L dof are then eliminated using static condensation yielding a three-node element with five engineering dof at each node; i.e., $\{u_i, v_i, w_i, \theta_{xi}, \theta_{yi}\}$ ($i = 1, 2, 3$) (see Figure 2).

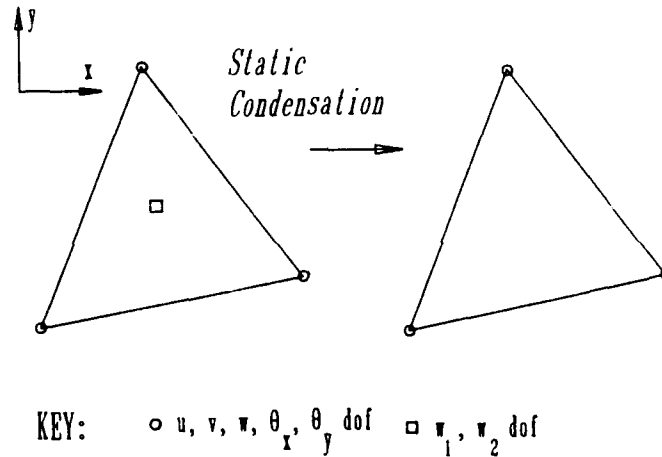


Figure 2. A three-node stretching-bending plate element with transverse shear and transverse normal deformation.

3.1.2 Shear Relaxation

The shear relaxation parameter, ϕ_s^2 , is a multiplier introduced in the transverse shear constitutive equations for the element

$$Q^L = \phi_s^2 G \gamma^L \quad (30)$$

The parameter is determined from the diagonal transverse shear, k_s^θ , and bending, k_b^θ , stiffness coefficients corresponding to rotational dof of the "unrelaxed" element stiffness matrix:¹⁵⁻¹⁸

$$\phi_s^2 = \frac{1}{1 + 2 (\sum k_s^\theta / \sum k_b^\theta)} \quad (31)$$

where the summations are carried over all six diagonal terms. The use of shear relaxation avoids locking in the thin regime.

The computer implementation of this three-node plate element, enabling its use with the general purpose finite element code ABAQUS, is discussed in Reference 31.

4. TRANSVERSE STRESS CALCULATIONS

Due to their heterogeneous nature, laminated composite plates generally exhibit ply-interface discontinuities in the inplane stresses, as well as in the transverse strains. Also, the inplane strains are continuous across the laminate thickness and the transverse stresses are also continuous, although their through-thickness gradients may be discontinuous at the ply interfaces.

Since the present theory relies upon continuous strain distributions across the entire laminate (as do all single-layer displacement theories), accurate inplane stresses can be recovered from the ply constitutive law (see Equation 5); however, the direct recovery of transverse stresses in this manner are often erroneous producing nonphysical discontinuities at the ply interfaces.

To obtain accurate, through-thickness continuous transverse shear stresses, one needs to integrate the three-dimensional equilibrium equations using the inplane stresses obtained from the constitutive relations (see Equation 5 and refer to Reference 8), that is

$$\begin{aligned} \sigma_{xz}^{(k)} &= - \int (\sigma_{xx,x}^{(k)} + \tau_{xy,y}^{(k)}) dz \\ &= - \int \left\{ \{ \tilde{C}_{11}, \tilde{C}_{12}, \tilde{C}_{13}, \tilde{C}_{16} \}^{(k)} \frac{\partial}{\partial x} \begin{bmatrix} \epsilon_{xx} \\ \epsilon_{yy} \\ \epsilon_{zz} \\ \gamma_{xy} \end{bmatrix} \right. \\ &\quad \left. + \{ \tilde{C}_{16}, \tilde{C}_{26}, \tilde{C}_{36}, \tilde{C}_{66} \}^{(k)} \frac{\partial}{\partial y} \begin{bmatrix} \epsilon_{xx} \\ \epsilon_{yy} \\ \epsilon_{zz} \\ \gamma_{xy} \end{bmatrix} \right\} dz. \end{aligned} \quad (31a)$$

$$\begin{aligned}
\sigma_{yz}^{(k)} &= - \int (\tau_{xy,x}^{(k)} + \sigma_{yy,y}^{(k)}) dz \\
&= - \int \left\{ \{ \tilde{c}_{16}, \tilde{c}_{26}, \tilde{c}_{36}, \tilde{c}_{66} \}^{(k)} \frac{\partial}{\partial x} \begin{bmatrix} \epsilon_{xx} \\ \epsilon_{yy} \\ \epsilon_{zz} \\ \gamma_{xy} \end{bmatrix} \right. \\
&\quad \left. + \{ \tilde{c}_{12}, \tilde{c}_{22}, \tilde{c}_{23}, \tilde{c}_{26} \}^{(k)} \frac{\partial}{\partial y} \begin{bmatrix} \epsilon_{xx} \\ \epsilon_{yy} \\ \epsilon_{zz} \\ \gamma_{xy} \end{bmatrix} \right\} dz
\end{aligned} \tag{31b}$$

where the strains are defined in Equation 7a and Equation 12. Having obtained the transverse shear stresses, the transverse normal stress, $\sigma_{zz}^{(k)}$, can be found either by integrating Equation 10 or applying Hooke's Law (see Equation 5). As will be shown in Section 5, in this plate theory both approaches yield accurate predictions for $\sigma_{zz}^{(k)}$; however, the Hooke's Law stress recovery yields slightly discontinuous transverse normal stresses at the ply interfaces.

While in the context of this plate theory, as well as others,⁸ the equilibrium stress-recovery approach has been effective; its application to the finite element method is not straightforward. For instance, in the case of the present finite element, all strain gradients in Equation 31 vanish identically (the strains are constant within the element domain); therefore, the direct utilization of these finite element strain gradients will always result in zero transverse shear stresses.

To overcome this difficulty, a global smoothing procedure^{27,28} yielding continuous solutions for the strains and their normal gradients across the entire plate domain was employed. The strain gradients were then used in Equation 31 to compute accurate through-thickness distributions of the transverse shear stresses. For complete details on the global smoothing procedure the reader is referred to Reference 28.

5. RESULTS AND DISCUSSION

Numerical studies are carried out for the problem of cylindrical bending of a carbon/epoxy symmetric angle-ply $([30/-30]_s)$ laminate subjected to a sinusoidal transverse pressure $q = q_0 \sin(\pi x/L)$ for which an exact elasticity solution is available²⁹ (see Figure 3a). This problem is rather challenging, exhibiting significant inplane shear coupling in each ply of the laminate. The ply material properties are taken as

$$\begin{aligned}
E_L &= 25 \times 10^6 \text{ psi}, & E_T &= 10^6 \text{ psi} \\
G_{LT} &= 0.5 \times 10^6 \text{ psi}, & G_{TT} &= 0.2 \times 10^6 \text{ psi} \\
\nu_{LT} &= \nu_{TT} = 0.25
\end{aligned} \tag{32}$$

where L and T denote the longitudinal and transverse ply material directions, respectively.

The results from the study were obtained analytically from the present Higher-Order Theory, shown as HOT-ANALYTIC (for the analytic solution approach refer to Reference 24), an exact elasticity approach,²⁹ designated as EXACT, the classical laminate plate theory (CPT), and the present finite element analysis, designated as HOT-FEM. Also, results corresponding to the shear-deformable version of the present theory (see Remarks 2.1) are presented and labeled in the figures as SHEAR-DEFORMABLE.

Figure 3b depicts a twenty-element finite element discretization of a narrow strip spanning one quarter of the loading wavelength (i.e., $L/2$). Appropriate symmetric boundary conditions and multiple-point kinematic constraint equations are enforced to simulate the cylindrical bending of the plate. In Figure 4, the percent error of the maximum midplane transverse displacement is plotted versus the half wavelength of loading-to-thickness ratio ($L/2h$). As $L/2h$ decreases, the observed deflection becomes dominated by transverse shear and transverse normal deformations. The thick regime improvement in accuracy afforded by the inclusion of both of these effects in the present theory is clearly evident.

The remainder of the discussion concerns the strain and stress predictions for the moderately thick ($L/2h = 10$) and thick ($L/2h = 4$) deformation regimes. Figures 5 and 6 depict through-thickness distributions of the maximum inplane (ϵ_{xx} and γ_{xy}) and transverse (γ_{xz} and ϵ_{zz}) strains, respectively. The observed departures from the exact elasticity solutions, particularly at the outer fibers for $L/2h = 4$, can be attributed to the linear distributions for u_x and u_y in the present theory. Note that their thickness variations according to the elasticity solution become increasingly nonlinear in the thick regime.

Figure 7 shows the distributions of the maximum transverse shear τ_{xz} and transverse normal σ_{zz} stresses. These stresses were computed following the conventional Hooke's Law stress recovery (see Equation 5), designated as HOT-HOOKE, and by integrating the three-dimensional equilibrium equations of elasticity (see Equation 31), designated as HOT-EQUIL. It is of interest to note that while the equilibrium-based transverse shear stress (τ_{xz}) recovery yielded superior results over those obtained from Hooke's Law, the transverse normal stress (σ_{zz}) recovery is highly accurate by both methods.

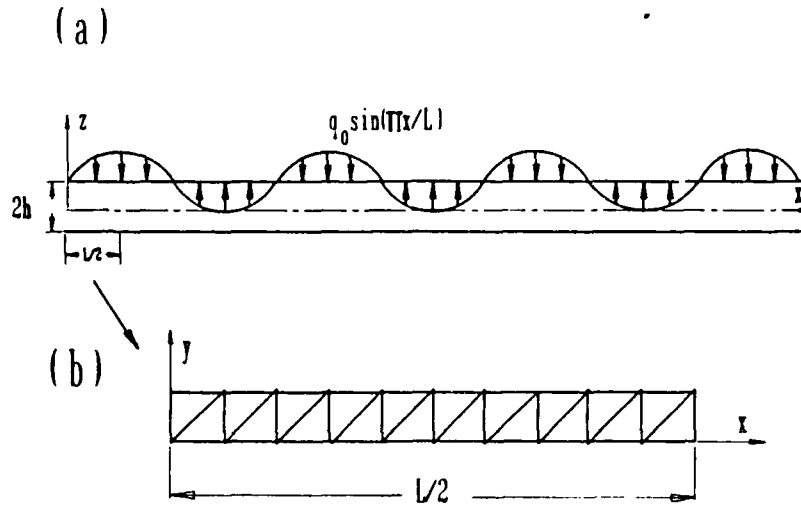


Figure 3. (a) Carbon/epoxy [30/-30]_s laminate subject to sinusoidal pressure in cylindrical bending; (b) finite element discretization.

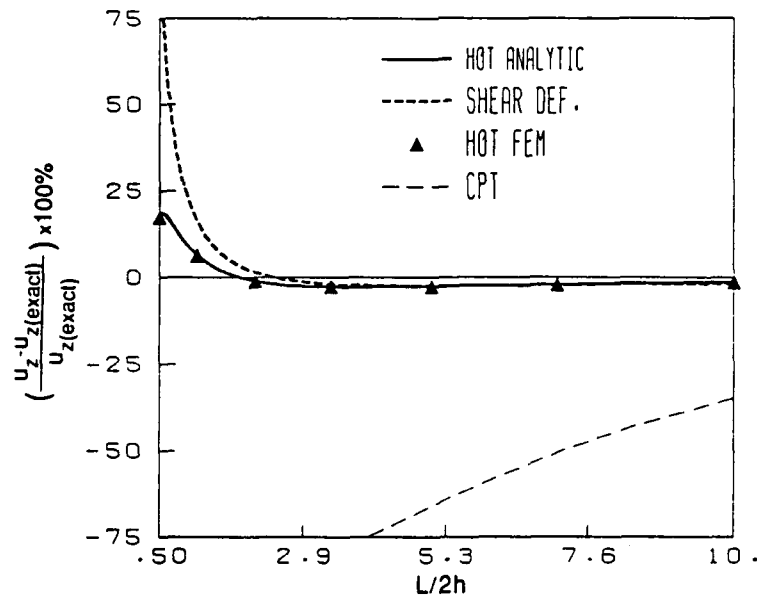


Figure 4. Percent error of maximum midplane deflection versus $L/2h$ ratio.

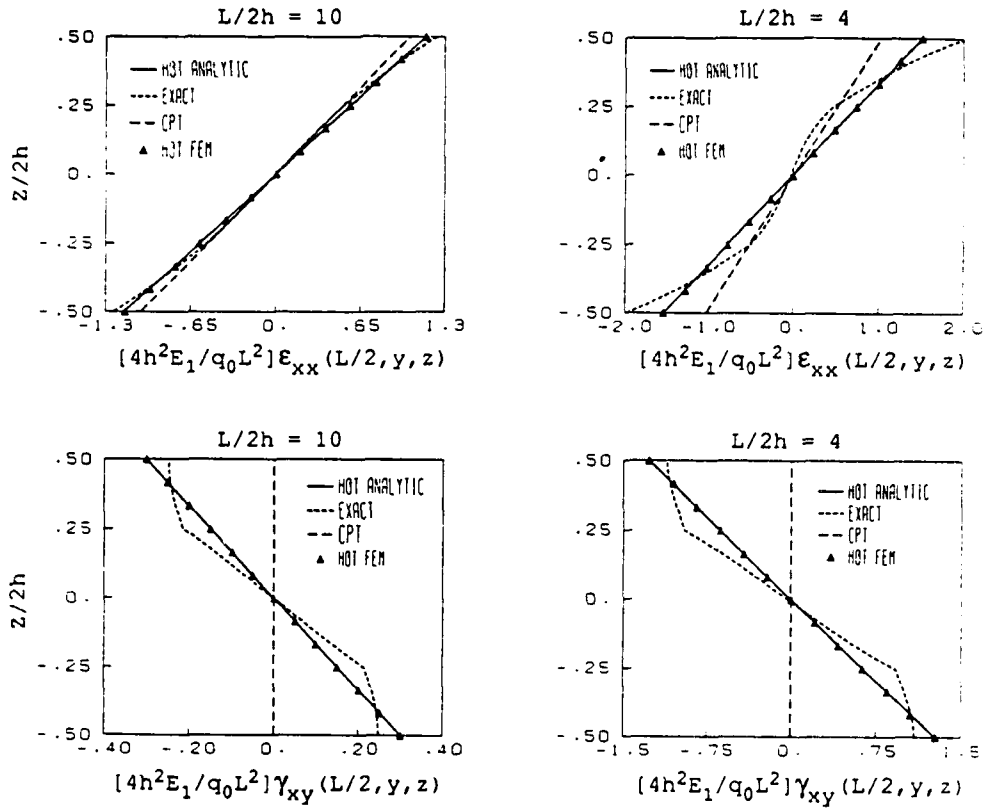


Figure 5. Distributions of inplane strains across thickness for $L/2h = 10$ and 4 .

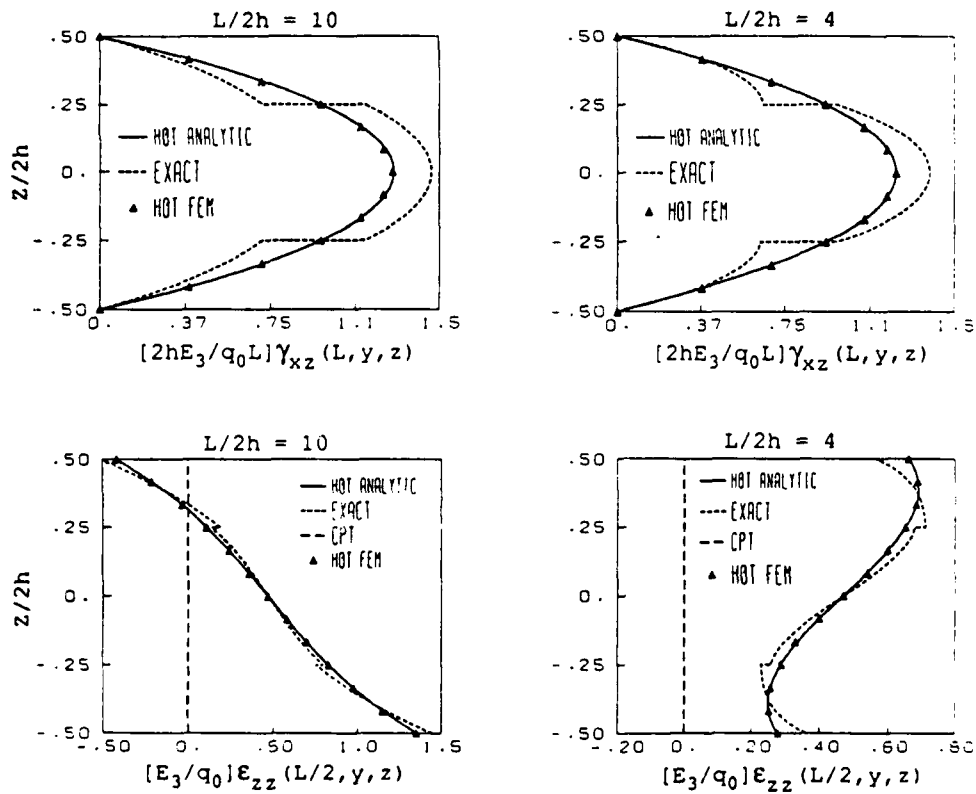


Figure 6. Distributions of transverse strains across thickness for $L/2h = 10$ and 4 .

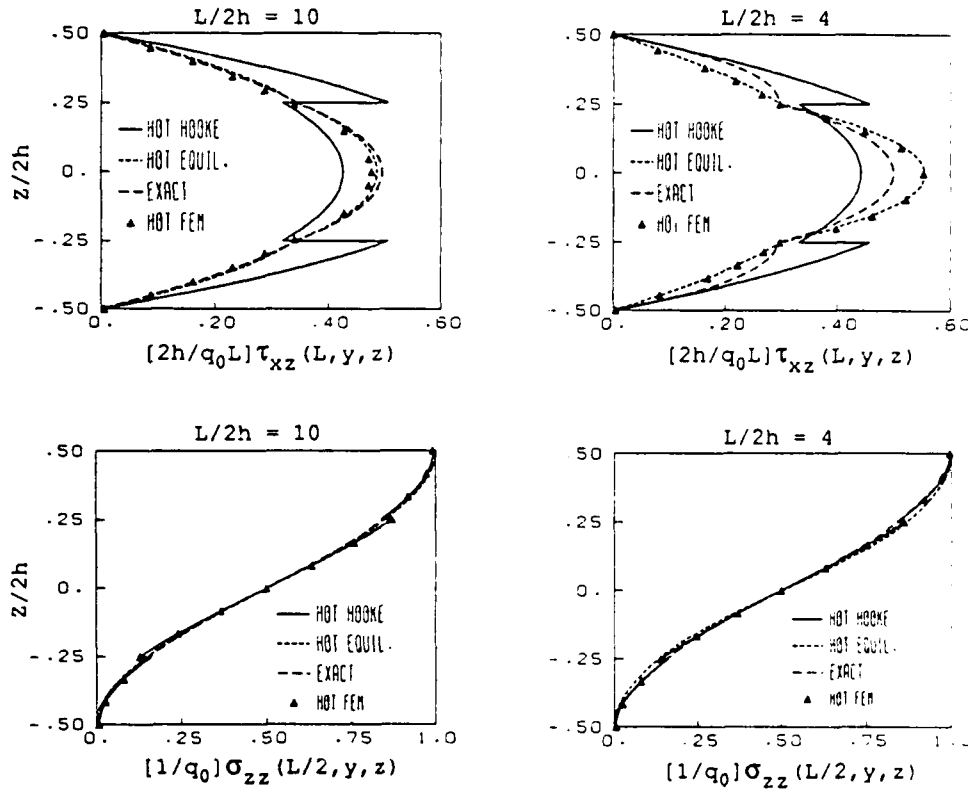


Figure 7. Distributions of transverse stresses across thickness for $L/2h = 10$ and 4.

6. CONCLUDING REMARKS

A computationally viable $\{1, 2\}$ higher-order plate theory for stress analysis of composite laminates was presented. The theory incorporates both transverse shear and transverse normal deformations and is based on linear through-thickness expansions for the inplane displacements and a special parabolic distribution for the transverse displacement. In addition, independent expansions were used for the transverse strains, satisfying exact transverse stress equilibrium at the top and bottom plate surfaces and having equivalent mean values to those obtained directly from the assumed displacements. From the three-dimensional virtual work principle, the two-dimensional plate variational principle is derived, giving rise to a coupled 10th-order stretching-bending theory subject to exclusively Poisson boundary conditions and two "auxiliary" 0th-order transverse stretching equations.

To demonstrate the theory's computational aspects, an efficient three-node stretching-bending plate element was developed. It was shown that the higher-order transverse displacements can be eliminated either directly from the variational statement or via static condensation at the element level. With the use of the latter approach, a 5-dof-per-node element was produced, having the same computational efficiency as a comparable first-order shear-deformable element. In addition, an effective approach for the recovery of reliable transverse stresses was discussed.

In closing, the practical benefits of the proposed laminate plate analysis are: (1) there are no requirements for "shear correction" factors; (2) reliable three-dimensional distributions of displacements, strains and stresses are attainable; (3) the range of applicability includes both thin- and thick-section composite laminates; and (4) the finite element formulation represents a viable enhancement over the widely used first-order shear-deformable models.

ACKNOWLEDGMENT

The authors wish to thank Colin Freese for utilizing the global smoothing technique²⁸ in the computations of transverse stresses.

APPENDIX A. PLATE STRESS RESULTANTS AND STRAINS

Stress Resultants

$$\mathbf{N}^T = \{N_x, N_y, N_z, N_{xy}\} = \sum_{k=1}^N \int_{h_{k-1}}^{h_k} \{\sigma_{xx}, \sigma_{yy}, \sigma_{zz}, \sigma_{xy}\}^{(k)} dz \quad (\text{A.1})$$

$$\mathbf{M}^T = \{M_x, M_y, M_z, M_{xy}\} = \sum_{k=1}^N \int_{h_{k-1}}^{h_k} \{(z\sigma_{xx}^{(k)} + \phi_1\sigma_{zz}^{(k)}), (z\sigma_{yy}^{(k)} + \phi_2\sigma_{zz}^{(k)}), \\ (\phi_3\sigma_{zz}^{(k)}), (z\tau_{xy}^{(k)} + \phi_6\sigma_{zz}^{(k)})\} dz \quad (\text{A.2})$$

$$\mathbf{Q}^T = \{Q_x, Q_y\} = \sum_{k=1}^N \int_{h_{k-1}}^{h_k} \frac{5}{4} (1 - \xi^2) \{\tau_{xz}^{(k)}, \tau_{yz}^{(k)}\} dz \quad (\text{A.3})$$

Plate Strains

$$\boldsymbol{\epsilon}^T = \{\epsilon_{x_0}, \epsilon_{y_0}, \epsilon_{z_0}, \gamma_{xy_0}\} = \{u_{,x}, v_{,y}, w_1/h, u_{,y} + v_{,x}\} \quad (\text{A.4})$$

$$\boldsymbol{\kappa}^T = \{\kappa_{x_0}, \kappa_{y_0}, \kappa_{z_0}, \kappa_{xy_0}\} = \{\theta_{y,x}, \theta_{x,y}, w_2/h^2, \theta_{x,x} + \theta_{y,y}\} \quad (\text{A.5})$$

$$\boldsymbol{\gamma}^T = \{\gamma_{xz_0}, \gamma_{yz_0}\} = \{w_{,x} + \theta_y, w_{,y} + \theta_x\} \quad (\text{A.6})$$

Applied Normal Traction

$$q_1 = q^+ - q^-, \quad q_2 = q^+ + q^- \quad (\text{A.7})$$

Prescribed Edge Stress Resultants

$$\{\bar{N}_{xn}, \bar{N}_{yn}\} = \int_{-h}^h \{\bar{T}_x, \bar{T}_y\} dz \quad (A.8)$$

$$\{\bar{M}_{xn}, \bar{M}_{yn}\} = \int_{-h}^h \{\bar{T}_x, \bar{T}_y\} z dz \quad (A.9)$$

$$\{\bar{Q}_{zn}, \bar{Q}_{z_1}, \bar{Q}_{z_2}\} = \int_{-h}^h \bar{T}_z \{1, \xi, \xi^2 - 1/5\} dz \quad (A.10)$$

Note: From (A.10), one can readily verify that the vanishing conditions on \bar{Q}_{zi} ($i = 1, 2$) in Equation 20 imply that \bar{T}_z must vary parabolically as $(1 - \xi^2)$ across the plate thickness.

APPENDIX B. PLATE CONSTITUTIVE RELATIONS

Invoking Hooke's Law (see Equation 5) into the plate stress resultants (Appendix A) yields the plate constitutive relations which can be expressed in matrix form as

$$\begin{bmatrix} \mathbf{N} \\ \mathbf{M} \\ \mathbf{Q} \end{bmatrix} = \begin{bmatrix} \mathbf{A} & \mathbf{B} & \mathbf{0} \\ \mathbf{B}^T & \mathbf{D} & \mathbf{0} \\ \mathbf{0} & \mathbf{0} & \mathbf{G} \end{bmatrix} \begin{bmatrix} \boldsymbol{\epsilon} \\ \boldsymbol{\kappa} \\ \boldsymbol{\gamma} \end{bmatrix} \quad (\text{B.1})$$

where the vectors of plate stress resultants and strains are defined in Appendix A; the constitutive matrices of elastic coefficients are:

Membrane Elastic Stiffness

$$\mathbf{A} = [\mathbf{A}_{ij}] \quad (i, j = 1, 2, 3, 6) \quad (\text{B.2})$$

where

$$A_{ij} = \sum_{k=1}^N \int_{h_{k-1}}^{h_k} C_{ij}^{(k)} dz$$

Membrane-Bending Coupling Elastic Stiffness

$$\mathbf{B} = [\mathbf{B}_{ij}] \quad (i, j = 1, 2, 3, 6), \quad (\text{B.3})$$

where

$$B_{iq} = \sum_{k=1}^N \int_{h_{k-1}}^{h_k} \left\{ C_{iq}^{(k)} z + C_{i3}^{(k)} \phi_q \right\} dz \quad (i = 1, 2, 3, 6; \quad q = 1, 2, 6)$$

$$B_{i3} = \sum_{k=1}^N \int_{h_{k-1}}^{h_k} C_{i3}^{(k)} \phi_3 dz \quad (i = 1, 2, 3, 6)$$

Bending Elastic Stiffness

$$D = [D_{ij}] \quad (i, j = 1, 2, 3, 6), \quad (B.4)$$

where

$$D_{qq} = \sum_{k=1}^N \int_{h_{k-1}}^{h_k} \left\{ C_{qq}^{(k)} z^2 + 2 C_{q3}^{(k)} \phi_q z + C_{33}^{(k)} \phi_q^2 \right\} dz \quad \text{for } q = 1, 2, 6$$

and

$$D_{33} = \sum_{k=1}^N \int_{h_{k-1}}^{h_k} C_{33}^{(k)} \phi_3^2 dz$$

$$D_{qr} = \sum_{k=1}^N \int_{h_{k-1}}^{h_k} \left\{ C_{qr}^{(k)} z^2 + (C_{q3}^{(k)} \phi_r + C_{r3}^{(k)} \phi_q) z + C_{33}^{(k)} \phi_q \phi_r \right\} dz$$

(q, r = 1, 2, 6)

$$D_{q3} = \sum_{k=1}^N \int_{h_{k-1}}^{h_k} \left\{ C_{q3}^{(k)} \phi_3 z + C_{33}^{(k)} \phi_q \phi_3 \right\} dz \quad (q = 1, 2, 6)$$

Transverse Shear Elastic Stiffness

$$G = [G_{ij}] \quad (i, j = 5, 4), \quad (B.5)$$

where

$$G_{ij} = \sum_{k=1}^N \int_{h_{k-1}}^{h_k} C_{ij}^{(k)} \left[\frac{5}{4} (1 - \xi^2) \right]^2 dz$$

REFERENCES

1. REISSNER, E. *On the Theory of Bending of Elastic Plates*. Journal of Mathematics and Physics, v. 23, 1944, p. 184-191.
2. REISSNER, E. *On a Variational Theorem in Elasticity*. Journal of Mathematics and Physics, v. 28-29, 1950, p. 90-95.
3. HILDEBRAND, F. B., REISSNER, E., and THOMAS, G. B. *Notes on the Foundations of the Theory of Small Displacements of Orthotropic Shells*. NACA TN, no. 1833, 1949.
4. MINDLIN, R. D. *Influence of Rotatory Inertia and Shear on Flexural Motions of Isotropic, Elastic Plates*. Journal of Applied Mechanics, v. 18, 1951, p. 31-38.
5. REISSNER, E. *Reflections on the Theory of Elastic Plates*. Appl. Mech. Review, v. 38, no. 11, 1985, p. 1453-1464.
6. REDDY, J. N. *On Refined Computational Models of Composite Laminates*. Int. J. Numer. Meths. Eng., v. 27, 1989, p. 361-382.
7. NOOR, A. K., and BURTON, W. S. *Assessment of Shear Deformable Theories for Multilayered Composite Plates*. Appl. Mech. Rev., v. 42, no. 1, 1989, p. 1-12.
8. LO, K. H., CHRISTENSEN, R. M., and WU, E. M. *Stress Solution Determination for Higher-Order Plate Theory*. Int. J. Solids and Structures, v. 14, 1978, p. 655-662.
9. REISSNER, E. *On a Certain Mixed Variational Theorem and a Proposed Application*. Int. J. Numer. Meths. Eng., v. 20, 1984, p. 1366-1368.
10. REISSNER, E. *On a Mixed Variational Theorem and on Shear Deformable Plate Theory*. Int. J. Numer. Meths. Eng., v. 23, 1986, p. 193-198.
11. SPILKER, R. L. *Hybrid Stress Formulations for Multilayer Isoparametric Plate Elements* in Finite Element Methods for Plate and Shell Structures, Vol. 1: Element Technology. T. J. R. Hughes and E. Hinton, eds., Pineridge Press, Swansea, U.K., 1986, p. 175-199.
12. YANG, P. C., NORRIS, C. H., and STAVSKY, Y. *Elastic Wave Propagation in Heterogeneous Plates*. Int. J. Solids Struct., v. 2, 1966, p. 665-684.
13. DONG, S. B., and TSO, F. K. W. *On a Laminated Orthotropic Shell Theory Including Transverse Shear Deformation*. J. Appl. Mech., v. 39, 1972, p. 1091-1097.
14. REDDY, J. N. *A Simple Higher-Order Theory for Laminated Composite Plates*. J. Appl. Mech., v. 45, 1984, p. 745-752.
15. TESSLER, A., and HUGHES, T. J. R. *A Three-Node Mindlin Plate Element with Improved Transverse Shear*. Comput. Meths. Appl. Mech. Eng., v. 50, 1985, p. 71-101.
16. TESSLER, A. *A Priori Identification of Shear Locking and Stiffening in Triangular Mindlin Elements*. Comput. Meths. Appl. Mech. Eng., v. 53, 1985, p. 183-200.
17. TESSLER, A. *A C^0 -anisoparametric Three-Node Shallow Shell Element*. Comput. Meths. Appl. Mech. Eng., v. 78, 1990, p. 89-103.
18. TESSLER, A. *Shear-Deformable Bending Elements with Penalty Relaxation* in Finite Element Methods for Plate and Shell Structures, Vol. 1: Element Technology. T. J. R. HUGHES and E. HINTON, eds., Pineridge Press, Swansea, U. K., 1986, p. 266-290.
19. HUGHES, T. J. R. *The Finite Element Method: Linear Static and Dynamic Finite Element Analysis*. Chapter 5, Prentice-Hall, Englewood Cliffs, NJ, 1987.
20. WHITNEY, J. M., and SUN, C. T. *A Refined Theory for Laminated Anisotropic, Cylindrical Shells*. Journal of Applied Mechanics, v. 41, 1974, p. 471-476.
21. NELSON, R. B., and LORCH, D. R. *A Refined Theory for Laminated Orthotropic Plates*. J. Appl. Mech., v. 41, 1974, p. 177-183.
22. LO, K. H., CHRISTENSEN, R. M., and WU, E. M. *A Higher-Order Theory of Plate Deformation*. Part 1: Homogeneous Plates, and Part 2: Laminated Plates. Journal of Applied Mechanics, v. 44, 1977, p. 663-676.
23. VALISETTY, R. R., and REHFELD, L. W. *A Theory for Stress Analysis of Composite Laminates*. Proc. 24th SDM Conf., AIAA Paper 83-0833-CP, 1983.
24. TESSLER, A. *A Higher-Order Plate Theory with Ideal Finite Element Suitability*. Comput. Meths. Appl. Mech. Eng. To be published, v. 85, 1991.
25. TESSLER, A. *A Higher-Order Plate Theory with Ideal Finite Element Suitability*. U.S. Army Materials Technology Laboratory, MTL TR 89-85, September 1989.
26. TESSLER, A. *An Improved Higher-Order Theory for Orthotropic Plates*. Proc. 13th Annual Composites Review, 1988, p. 59-65.
27. TESSLER, A., FREESE, C., ANASTASI, R., SERABIAN, S., OPLINGER, D., and KATZ, A. *Least-Squares Penalty-Constraint Finite Element Method for Generating Strain Fields From Moire Fringe Patterns*. Photomechanics And Speckle Metrology. SPIE Vol. 814, 1987, p. 314-323.
28. TESSLER, A., and FREESE, C. *A Global Penalty-Constraint Finite Element Formulation for Effective Strain and Stress Recovery*. Presented at the 8th Army Conference on Applied Mathematics and Computing, Cornell University, 1990.
29. PAGANO, N. J. *Influence of Shear Coupling in Cylindrical Bending of Anisotropic Laminates*. J. Composite Materials, v. 4, 1970, p. 330-343.
30. LEIKNITSKII, S. G. *Theory of Elasticity of an Anisotropic Elastic Body*. Holden-Day, Oakland, CA, 1963.
31. SAETHER, E., and TESSLER, A. *User-Defined Subroutine Interface for use of HLOT3 Plate Element in ABAQUS*, U. S. Army Materials Technology Laboratory, MTL TR (to appear in 1991).

DISTRIBUTION LIST

No. of Copies	To
1	Office of the Under Secretary of Defense for Research and Engineering, The Pentagon, Washington, DC 20301
1	Commander, U.S. Army Materiel Command, 5001 Eisenhower Avenue, Alexandria, VA 22333-0001 ATTN: AMCLD
1	Commander, U.S. Army Laboratory Command, 2800 Powder Mill Road, Adelphi, MD 20703-1145 ATTN: AMSLC-IM-TL
1	AMSLC-CT
2	Commander, Defense Technical Information Center, Cameron Station, Building 5, 5010 Duke Street, Alexandria, VA 22304-6145 ATTN: DTIC-FDAC
1	Metals and Ceramics Information Center, Battelle Columbus Laboratories, 505 King Avenue, Columbus, OH 43201
1	Commander, Army Research Office, P.O. Box 12211, Research Triangle Park, NC 27709-2211 ATTN: Information Processing Office
1	Commander, U.S. Army Electronics Technology and Devices Laboratory, Fort Monmouth, NJ 07703-5000 ATTN: SLCET-DT
1	Commander, U.S. Army Missile Command, Redstone Arsenal, AL 35898-5247 ATTN: AMSMI-RD-ST
1	Technical Library
2	Commander, U.S. Army Armament, Munitions and Chemical Command, Dover, NJ 07801 ATTN: SMCAR-TDC
1	Commander, U.S. Army Natick Research, Development and Engineering Center, Natick, MA 01760-5010 ATTN: Technical Library
1	Commander, U.S. Army Tank-Automotive Command, Warren, MI 48397-5000 ATTN: AMSTA-R
1	Commander, U.S. Army Engineer Waterways Experiment Station, P.O. Box 631, Vicksburg, MS 39180 ATTN: Research Center Library
1	Director, U.S. Army Ballistic Research Laboratory, Aberdeen Proving Ground, MD 21005 ATTN: SLCBR-DD-T (STINFO)
1	SLCBR-IV-M, Dr. W. H. Drysdale
1	SLCBR-TB-W, Dr. J. Walter
1	Director, Benet Weapons Laboratory, LCWSL, USA AMCCOM, Watervliet, NY 12189 ATTN: AMSMC-LCB-TL
3	Commander, U.S. Army Foreign Science and Technology Center, 220 7th Street, N.E., Charlottesville, VA 22901-5396 ATTN: AIFRTC, Applied Technologies Branch, Gerald Schlesinger
1	Commander, U.S. Army Aviation Systems Command, Aviation Research and Technology Activity, Aviation Applied Technology Directorate, Fort Eustis, VA 23604-5577 ATTN: SAVDL-E-MOS
1	Director, Langley Directorate, U.S. Army Air Mobility Research and Development Laboratory, NASA-Langley Research Center, Hampton, VA 23665 ATTN: Aerostructures Directorate
1	Naval Research Laboratory, Washington, DC 20375 ATTN: Code 5830
1	Office of Naval Research, 800 North Quincy Street, Arlington, VA 22217-5000 ATTN: Mechanics Division, Code 1132-SM

No. of Copies	To
1	U.S. Navy David Taylor Research Center, Bethesda, MD 20084 ATTN: Code 172
1	U.S. Air Force Office of Scientific Research, Bolling Air Force Base, Washington, DC 20332 ATTN: Mechanics Division
1	Commander, U.S. Air Force Wright Research & Development Center, Wright-Patterson Air Force Base, OH 45433-6523 ATTN: WRDC/MLLN
1	NASA - Marshall Space Flight Center, MSFC, AL 35812 ATTN: EH01, Dir, M&P lab
1	Committee on Marine Structures, Marine Board, National Research Council, 2101 Constitution Avenue, N.W., Washington, DC 20418
1	U.S. Army Research Office, P.O. Box 12211, Research Triangle Park, NC 27709 ATTN: Dr. Robert Singleton
1	Dr. Gary L. Anderson, Chief, Structures and Dynamics Branch, Engineering Sciences Division
1	NASA - Langley Research Center, U.S. Army Aerostructures Directorate, USAARTA, Hampton, VA 23665-5225 ATTN: Dr. Wolf Elber, MS 266
1	NASA - Langley Research Center, Hampton, VA 23665 ATTN: H. L. Bohon, MS 243
1	George Washington University Center - at NASA - Langley Research Center, Hampton, VA 23665 ATTN: Professor A. K. Noor, Mail Stop 246C
1	NASA/GSFC, Greenbelt, MD 20771 ATTN: Mr. William Case, Mail Code 725
1	Ship and Submarine Materials Technology, DTRC-0115, Annapolis, MD 21402 ATTN: Mr. Ivan L. Caplan
1	Director, Structures Directorate, USA MICOM, Redstone Arsenal, AL 35898 5247 ATTN: AMSMI-RD-ST, Dr. Larry C. Mixon
1	Benet Laboratories, Watervliet Arsenal, Watervliet, NY 12189-4050 ATTN: Dr. Giuliano D'Andrea, Chief, Research Division
1	Dr. John Vasilakis, Chief, Applied Mechanics Branch
1	Office of Naval Research, Solid Mechanics Program, 800 North Quincy Street, Arlington, VA 22217-5000 ATTN: Dr. Roshdy Barsoum, Code 1132
1	Massachusetts Institute of Technology, Department of Mechanical Engineering, Cambridge, MA 02139 ATTN: Professor K. J. Bathe
1	Professor David Parks
1	Massachusetts Institute of Technology, Department of Astronautics and Aeronautics, Building 73, Room 311, Cambridge, MA 02139 ATTN: Professor Ted H. H. Pian
1	Professor S. N. Atluri, Director, Center for the Advancement of Computational Mechanics, Georgia Institute of Technology, Mail Code 0356, Atlanta, GA 30332
1	Dr. Lawrence C. Bank, The Catholic University of America, Department of Civil Engineering, Washington, DC 20064

No. of Copies	To
1	Professor Ted Belytschko, Northwestern University, Department of Civil Engineering, Evanston, IL 60201
1	Professor Fu-Kuo Chang, Stanford University, Department of Aeronautics and Astronautics, Stanford, CA 94305
1	Professor Tse-Yung P. Chang, The University of Akron, Department of Civil Engineering, Akron, OH 44325
1	Dr. Sailendra N. Chatterjee, Materials Sciences Corporation, 930 Harvest Drive, Suite 300, Blue Bell, PA 19422
1	Professor Thomas J. R. Hughes, Stanford University, Division of Applied Mechanics, Durand Building, Stanford, CA 94305
1	Professor S. W. Lee, University of Maryland, Department of Aerospace Engineering, College Park, MD 20742
1	Professor Alan J. Levy, Syracuse University, Department of Mechanical and Aerospace Engineering, 139 E. A. Link Hall, Syracuse, NY 13244-1240
1	Professor J. N. Reddy, Virginia Polytechnic Institute and State University, College of Engineering, Department of Engineering Science and Mechanics, Blacksburg, VA 24061-0219
1	Professor L. W. Rehfield, University of California at Davis, Department of Mechanical Engineering, Davis, CA 95616
1	Professor Eric Reissner, University of California at San Diego, Department of Applied Mechanics and Engineering Science, LaJolla, CA 92093
1	Professor John N. Rossettos, Northeastern University, College of Engineering, Department of Mechanical Engineering, 360 Huntington Avenue, Boston, MA 02115
1	Professor J. C. Simo, Stanford University, Division of Applied Mechanics, Stanford, CA 94305
1	R. L. Spilker, Rensselaer Polytechnical Institute, Department of Mechanical Engineering, Aeronautical Engineering and Mechanics, Troy, NY 12181
1	Dr. G. M. Stanley, Lockheed Palo Alto Research Laboratory, Mechanics of Materials Engineering, Palo Alto, CA 94304
1	Mr. Joseph R. Soderquist, Federal Aviation Administration, 800 Independence Ave., S.W., Washington, DC 20591
1	Mr. D. Erich Weerth, FMC Corporation, MD P95, 2890 De La Cruz Blvd, Box 58123, Santa Clara, CA 95052
1	Dr. E. T. Camponeschi, David Taylor Research Center, Code 2802, Annapolis, MD 21402
1	Dr. John H. Bode, Honeywell Armament Systems Division, 7225 Northland Dr., Brooklyn Park, MN 55428
1	Dr. Paul A. Lagace, Massachusetts Institute of Technology, Room 33-303, 77 Massachusetts Ave., Cambridge, MA 02139
1	Mr. Terry L. Vandiver, U.S. Army Missile Command, ATTN: AMSMI-RD-ST-CM, Redstone Arsenal, AL 35898-5247
1	Mr. Peter Shyprykevich, Grumman Aircraft Systems, MS B44-35, Bethpage, NY 11714
1	Professor Isaac Fried, Mathematics Department, Boston University, Boston, MA 02215
1	Professor C. A. Felippa, Department of Aerospace Engineering Sciences and Center for Space Structures and Controls, University of Colorado, Boulder, CO 80309-0429

No. of Copies	To
1	Professor A. F. Saleeb, Department of Civil Engineering, University of Akron, Akron, OH 44325
1	Professor Stanley B. Dong, Department of Civil Engineering, University of California, Los Angeles, CA 90024
1	Professor Richard B. Nelson, Department of Civil Engineering, University of California, Los Angeles, CA 90024
1	Dr. R. Badaliane, ATTN: Code 6380, Naval Research Laboratory, Washington, DC 20375
1	Mr. A. D. Carlson, Engineering Mechanics Division, Naval Underwater Systems Center, New London, CT 06320
	Director, U.S. Army Materials Technology Laboratory, Watertown, MA 02172-0001
2	ATTN: SLCMT-TML
2	Authors

U.S. Army Materials Technology Laboratory
Watertown, Massachusetts 02172-0001
A COMPUTATIONALLY VIABLE HIGHER-ORDER
THEORY FOR LAMINATED COMPOSITE PLATES -
Alexander Tessler and Erik Saether

AD UNCLASSIFIED
UNLIMITED DISTRIBUTION
Key Words

Technical Report MTL TR 90-59, November 1990, 28 pp-
illus,
Higher-order plate theory
Transverse shear deformation
Transverse normal deformation

A variational higher-order theory involving all transverse strain and stress components is proposed for the analysis of laminated composite plates. Derived from three-dimensional elasticity with emphasis on developing a viable computational methodology, the theory is well suited for finite element approximations as it incorporates both C^0 and C^1 continuous kinematic fields and Poisson boundary conditions. From the theory, a simple three-node stretching-bending finite element is developed and applied to the problem of cylindrical bending of a symmetric carbon/epoxy laminate for which an exact solution is available. Both the analytic and finite element results were found to be in excellent agreement with the exact solution for a wide range of the length-to-thickness ratio. The proposed higher-order theory has the same computational advantages as first-order shear-deformable theories. The present methodology, however, provides greater predictive capability, especially, for thick-section composites.

U.S. Army Materials Technology Laboratory
Watertown, Massachusetts 02172-0001
A COMPUTATIONALLY VIABLE HIGHER-ORDER
THEORY FOR LAMINATED COMPOSITE PLATES -
Alexander Tessler and Erik Saether

AD UNCLASSIFIED
UNLIMITED DISTRIBUTION
Key Words

Technical Report MTL TR 90-59, November 1990, 28 pp-
illus,
Higher-order plate theory
Transverse shear deformation
Transverse normal deformation

A variational higher-order theory involving all transverse strain and stress components is proposed for the analysis of laminated composite plates. Derived from three-dimensional elasticity with emphasis on developing a viable computational methodology, the theory is well suited for finite element approximations as it incorporates both C^0 and C^1 continuous kinematic fields and Poisson boundary conditions. From the theory, a simple three-node stretching-bending finite element is developed and applied to the problem of cylindrical bending of a symmetric carbon/epoxy laminate for which an exact solution is available. Both the analytic and finite element results were found to be in excellent agreement with the exact solution for a wide range of the length-to-thickness ratio. The proposed higher-order theory has the same computational advantages as first-order shear-deformable theories. The present methodology, however, provides greater predictive capability, especially, for thick-section composites.

U.S. Army Materials Technology Laboratory
Watertown, Massachusetts 02172-0001
A COMPUTATIONALLY VIABLE HIGHER-ORDER
THEORY FOR LAMINATED COMPOSITE PLATES -
Alexander Tessler and Erik Saether

AD UNCLASSIFIED
UNLIMITED DISTRIBUTION
Key Words

Technical Report MTL TR 90-59, November 1990, 28 pp-
illus,
Higher-order plate theory
Transverse shear deformation
Transverse normal deformation

A variational higher-order theory involving all transverse strain and stress components is proposed for the analysis of laminated composite plates. Derived from three-dimensional elasticity with emphasis on developing a viable computational methodology, the theory is well suited for finite element approximations as it incorporates both C^0 and C^1 continuous kinematic fields and Poisson boundary conditions. From the theory, a simple three-node stretching-bending finite element is developed and applied to the problem of cylindrical bending of a symmetric carbon/epoxy laminate for which an exact solution is available. Both the analytic and finite element results were found to be in excellent agreement with the exact solution for a wide range of the length-to-thickness ratio. The proposed higher-order theory has the same computational advantages as first-order shear-deformable theories. The present methodology, however, provides greater predictive capability, especially, for thick-section composites.

U.S. Army Materials Technology Laboratory
Watertown, Massachusetts 02172-0001
A COMPUTATIONALLY VIABLE HIGHER-ORDER
THEORY FOR LAMINATED COMPOSITE PLATES -
Alexander Tessler and Erik Saether

AD UNCLASSIFIED
UNLIMITED DISTRIBUTION
Key Words

Technical Report MTL TR 90-59, November 1990, 28 pp-
illus,
Higher-order plate theory
Transverse shear deformation
Transverse normal deformation

A variational higher-order theory involving all transverse strain and stress components is proposed for the analysis of laminated composite plates. Derived from three-dimensional elasticity with emphasis on developing a viable computational methodology, the theory is well suited for finite element approximations as it incorporates both C^0 and C^1 continuous kinematic fields and Poisson boundary conditions. From the theory, a simple three-node stretching-bending finite element is developed and applied to the problem of cylindrical bending of a symmetric carbon/epoxy laminate for which an exact solution is available. Both the analytic and finite element results were found to be in excellent agreement with the exact solution for a wide range of the length-to-thickness ratio. The proposed higher-order theory has the same computational advantages as first-order shear-deformable theories. The present methodology, however, provides greater predictive capability, especially, for thick-section composites.